Simplified Constitutive Model for Fatigue Behavior of Concrete in Compression

Benard Isojeh[1]; Maria El-Zeghayar, Ph.D.[2]; and Frank J. Vecchio, Ph.D., P.Eng.[3]

Abstract: In the literature, three basic assumptions are used to modify monotonic constitutive models in order to simplify fatigue analysis of concrete. First, the fatigue hysteresis loop at failure is assumed to intersect the monotonic stress–strain envelope. Second, it is assumed that the peak stress of a fatigue-damaged concrete element intersects the monotonic stress–strain envelope. Third, the centerlines of fatigue hysteresis loops are assumed to converge at a common point. Although the modifications supposedly lead to improved predictions, experimental verifications of these assumptions are currently insufficient to justify their implementation in the fatigue analysis of complex and large concrete structures where considerations of safety and cost-effectiveness are expedient. From experimental verifications conducted to ascertain the conservative level of these assumptions, it was found that the first and second assumptions seem reasonable, while the third assumption was inaccurate and thus in need of improvement. As such, a new convergence point is proposed. The constitutive models for high-strength and normal-strength concrete in compression were also modified as functions of the irreversible strain and residual strength. Further, a model was proposed for the irreversible strain accumulation, and its corroboration with experimental results showed good agreement. **DOI:** [10.1061/(ASCE)MT.1943-5533.0001863.](10.1061/(ASCE)MT.1943-5533.0001863) © *2017 American Society of Civil Engineers.*

Introduction

In the design of fatigue-prone concrete structures, fatigue-life models for concrete are used to verify the resistance of critical components. Basically, this verification ensures that fatigue failure will not occur during service life (Su and Hsu 1988).

One such model used is the stress-life model (*S-N* curve). An *S-N* curve is a plot of normalized stresses (with material strength) against the corresponding numbers of cycles at which failure occurs. Provided that the induced stress in the concrete element, corresponding ultimate strength, and other influencing factors such as frequency are taken into consideration, the number of cycles to failure can be estimated.

Investigations conducted on the influence of frequency on the fatigue life of concrete by Sparks and Menzies (1973), Raithby and Galloway (1974), Holmen (1982), Zhang et al. (1996), and Medeiros et al. (2015) all indicated that the number of cycles leading to failure decreases as the frequency of loading decreases. This behavior has been observed to be more pronounced as the maximum fatigue stress level increases (Torrenti et al. 2010).

Although the influence of loading parameters can be observed in the estimated number of cycles leading to failure, stress-life models do not account for the progressive degradation of concrete properties under fatigue loading. Hence, the corresponding influence of frequency in progressive damage cannot be observed (Zanuy et al. 2007; Tamulenas and Gelazius 2014). In order to account for the progressive degradation of concrete, two alternative approaches have been used.

In the first approach, certain assumptions are made for the relationship between monotonic stress–strain envelopes and evolving fatigue hysteresis loops. One such assumption is that the failure of a concrete specimen occurs at the instant when a fatigue stress–strain hysteresis loop intersects the softening portion of a monotonic stress–strain curve (Fig. 1) (Karsan and Jirsa 1969; Otter and Naaman 1989; Cachim et al. 2002; Petryna et al. 2002; Torrenti et al. 2010). In subsequent sections, the monotonic stress–strain curve will be referred to as the stress–strain envelope.

The peak stress point from a fatigue-damaged stress–strain curve is also assumed to intersect the descending portion of the stress–strain envelope (Petryna et al. 2002; Xiang and Zhao 2007). From this assumption, a constitutive model that considers the damage evolution of concrete residual strength can be developed for concrete.

According to Park (1990), the centerlines of hysteresis loops always pass through a common point irrespective of the stress level or stress range. Similarly, Xiang and Zhao (2007) also assumed that the initial tangential moduli of a damaged concrete element meet at a common point, although different from the point assumed by Park (1990).

In Fig. 1, ε, ε_d, and E_{fat} are the total strain, irreversible strain, and fatigue secant modulus, respectively. Provided damage evolution models for any two of the parameters (total strain, irreversible strain, and fatigue secant modulus) are known, the damage evolution of an unknown parameter can be developed using the assumptions (Park 1990; Xiang and Zhao 2007; Torrenti et al. 2010).

Analytical results reported in the literature using the aforementioned approach and assumptions are acceptable (Park 1990; Eligehausen et al. 1992; Petryna et al. 2002; Xiang and Zhao 2007; Zuradzka 2008). However, available experimental reports on these assumptions are insufficient to ascertain their validity and to justify their conservative form in fatigue analysis of concrete structures.

The second approach involves the use of damage mechanics based on thermodynamics of irreversible processes. In this approach, a damage variable or matrix is used to represent microcracks and

[1]Ph.D. Candidate, Dept. of Civil Engineering, Univ. of Toronto, Toronto, ON, Canada M5S 1A4 (corresponding author). ORCID: http://orcid.org/0000-0002-5095-5134. E-mail: mb.isojeh@mail.utoronto.ca

[2]Civil Engineer, Renewable Power Business Unit, Hatch Ltd., Niagara falls, ON, Canada L2E 7J7.

[3]Professor, Dept. of Civil Engineering, Univ. of Toronto, Toronto, ON, Canada M5S 1A4.
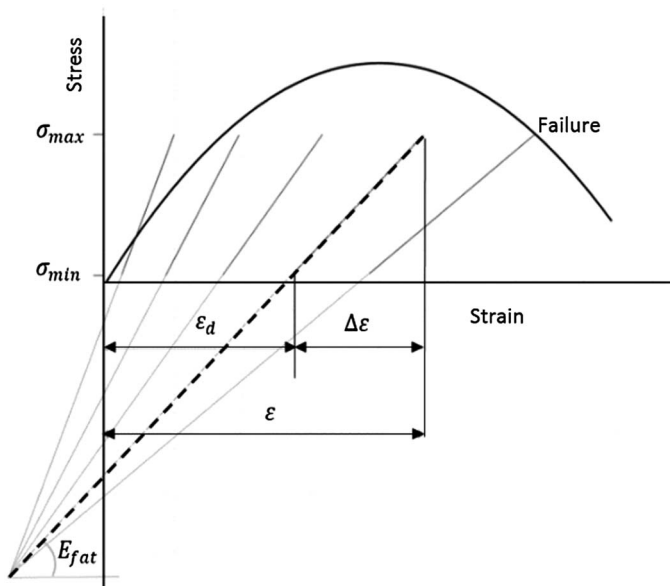
Fig. 1. Relationship between monotonic stress–strain curve and fatigue hysteresis loops

microvoids. The damage matrix may be assumed to depend on the orthotropic nature of fatigue microcracks (Chaboche 1981, 1988a, b; Lemaitre 1986; Lemaitre and Chaboche 1990; Vega et al. 1995; Zhang and Cai 2010).

The damage strain-energy release rate required in this approach is derived from the strain energy with respect to the damage variable. In addition, the elastic strain is derived from the strain energy with respect to the applied stress.

A damage-evolution function can be developed based on an incremental theory of plasticity in which multiple surfaces in stress space or strain-energy release space are defined (Dafalias and Popov 1977; Suaris et al. 1990; Al-Gadhib et al. 2000). However, a simplified concept that involves experimental data and a phenomenological approach can also been implemented to obtain models for damage evolution (Vega et al. 1995).

Verification studies via experiments with models developed from the second approach have also shown acceptable predictions. However, the approach involves extensive analysis. Since concrete is not homogeneous, constant and sufficient accuracy using this approach cannot be guaranteed. Further, the implementation of other salient factors in the derived fatigue-damage-evolution models and the modification of the approach for variable fatigue loading will require more assumptions and further complexity in analysis.

In this paper, the assumptions reported in the literature are verified experimentally and a constitutive model for concrete elements under fatigue loading in compression is developed. The irreversible strain accumulation required in the constitutive model is proposed as a function of the residual strength and fatigue secant modulus damage. The damage models for concrete strength and secant modulus used in the irreversible strain and constitutive models have been developed previously (Isojeh et al. 2016; Isojeh 2016).

Experimental Study

Tests were conducted in order to verify the three basic assumptions used for simplifying the behavior of concrete under fatigue loading. Monotonic tests were initially conducted on concrete cylindrical specimens in order to obtain the average compressive strength. Thereafter, percentages of the average strength were used as fatigue loads.

In the first group of fatigue tests, 22 specimens were tested to different numbers of cycles at a constant stress level and subsequently subjected to monotonic loading. The obtained stress–strain curves from monotonic loading were plotted alongside the stress–strain envelope to observe the intersection of the peak stress of the stress–strain curves with the softening portion of the stress–strain envelope.

In the second group of fatigue tests, 16 specimens were tested to failure under constant fatigue loading, and the hysteresis loops were plotted. The centerline of each loop was extended in order to observe a convergence point. The intersection of the hysteresis loop at failure with the stress–strain envelope was also verified. The tests procedures, the specimen tests, and the observations are discussed subsequently.
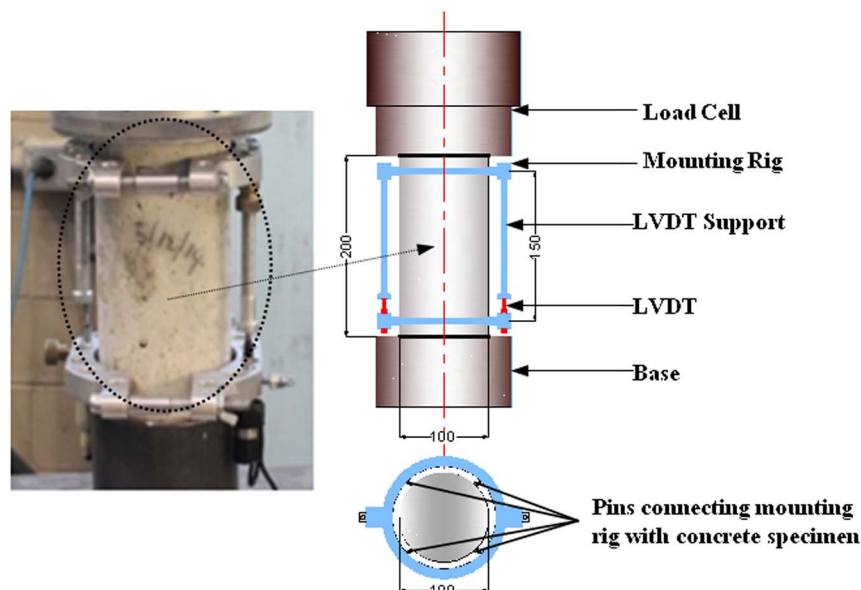
Fig. 2. Fatigue loading setup

Table 1. Average Compressive Strength and Corresponding Strain

Batch (number of specimens)	Average compressive strength (MPa)	Average corresponding strain (×0.001)	Mix ratio
1 (5)	52.8	2.01	1:2:2
2 (3)	55.8	2.00	1:2:2
3 (3)	46.2	1.95	1:2:3
4 (3)	23.1	1.52	1.2.4

Table 2. Percentage of Average Compressive Strength for Fatigue Loading

Batch (number of specimens)	% of average compressive strength (MPa)	Average compressive strength (MPa)	Frequency (Hz)
1 (5)	74	52.8	5
1 (2)	69	52.8	5
2 (2)	80	55.8	5
3 (2)	74	46.2	5
4 (2)	75	23.1	5
4 (3)	75	23.1	1

Servohydraulic testing equipment with a loading capacity of 1,000 kN was used to conduct fatigue tests on concrete cylinders (100 mm diameter × 200 mm height). In all tests, the waveform of the applied fatigue loading was sinusoidal in nature. In order to measure the progressive average strains throughout the tests, LVDTs were mounted on opposite sides of each specimen. Fig. 2 shows the tests set-up and LVDTs attached to a concrete specimen.

Test Specimens

The concrete specimens were made from portland cement (general use, GU), sand, and limestone aggregates (10 mm maximum size) with three different mix ratios. The concrete from the first two batches (Table 1), were cast using a mix proportion of 1:2:2 with water/cement ratio of 0.5, indicating cement, sand, and coarse aggregate respectively. Mix proportion ratios of 1:2:3 with water/cement ratio of 0.5 and 1:2:4 with water/cement ratio of 0.6 were used for the third and fourth batches, respectively. The static strengths of concrete after curing for 28 days were obtained for each batch (Table 1), while fatigue tests were conducted 30–40 days after casting.

Percentages of the average compressive strengths of the four batches (69–80%) were used as maximum stress levels for fatigue tests conducted on 16 specimens to failure (Table 2). The 22 specimens loaded to different numbers of cycles less than the number of cycles leading to failure at a constant maximum stress level of 0.74 (Table 3) and a frequency of 5 Hz are given in Table 3. The residual strengths and secant moduli of the specimens after monotonic loading to failure are also given in Table 3. A constant minimum load of 5 kN was used for all the tests conducted. The approach for estimating the fatigue secant modulus will be discussed in a subsequent section.

The progressive strain readings of the 16 concrete cylinders (100 mm diameter × 200 mm height) tested under uniaxial constant fatigue loading in compression were obtained using a data-acquisition system.

The 16 specimens tested to failure were used to verify Park's (1990) assumption and that of the intersection of the hysteresis loop with the stress–strain envelope at failure. The 22 specimens tested to different numbers of cycles before failure were used to verify the assumption of the intersection of the peak stress with the softening portions of the stress–strain envelope.

The servohydraulic testing equipment used was unable to capture the softening of concrete properly after attaining peak strength due to the stiffness of the material testing systems (MTS) setup used; hence, the average compressive strength and corresponding average peak strain values obtained from monotonic tests were substituted into Popovics' (1970) and Hognestad's (1951) stress–strain equations for high-strength and normal-strength concrete, respectively. The stress–strain curves generated were used as

Table 3. Strength and Secant Modulus Degradation Test Data

Specimen	Initial compressive strength f'_c	Number of cycles before static loading	Residual strength after static loading (MPa)	Residual fatigue modulus (MPa)	Corresponding static secant modulus (MPa)
E22	52.8	430	54.9	68,869	41,905
E9	52.8	430	54.4	58,088	38,537
E20	52.8	860	55.1	65,124	40,204
E11	52.8	860	53	58,806	37,101
E4	52.8	5,150	55.3	62,047	39,010
E17	52.8	7,730	52.3	55,211	35,000
E1	52.8	8,160	53.4	53,333	35,475
ST2	52.8	3,480	46.5	44,222	30,498
G3	46.2	5,550	41.7	33,433	23,496
G7	46.2	5,880	38.6	30,136	21,553
G8	46.2	18,080	36.3	31,402	21,889
G9	46.2	6,180	32.9	25,759	17,560
H1	55.8	5,000	51.4	50,244	31,815
H3	55.8	1,200	58.1	61,804	39,710
H9	55.8	3,000	56.2	57,622	36,786
H4	55.8	6,120	45.6	45,055	29,182
H5	55.8	5,840	49.2	43,871	28,834
H6	55.8	7,900	44.7	42,842	28,264
H7	55.8	4,680	36.1	37,169	[a]
H11	55.8	6,710	52.5	54,342	34,561
H14	55.8	9,870	46.8	38,750	26,689
H15	55.8	8,660	37.9	33,306	[a]

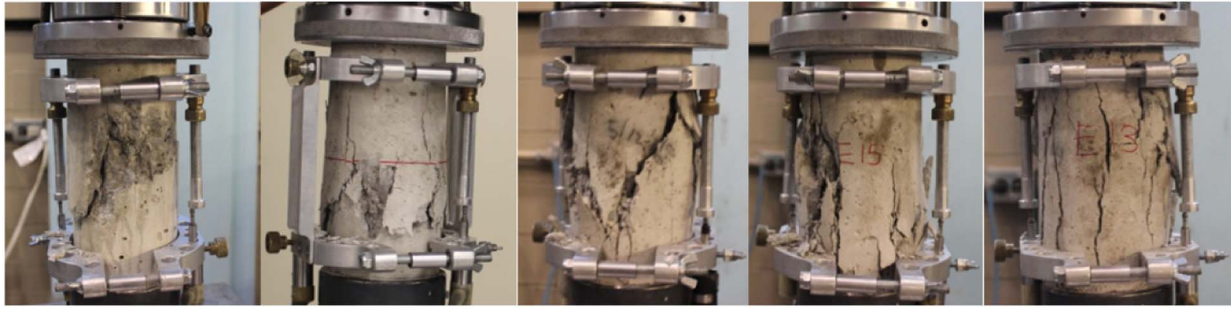[a]Failed before reaching maximum fatigue load applied.
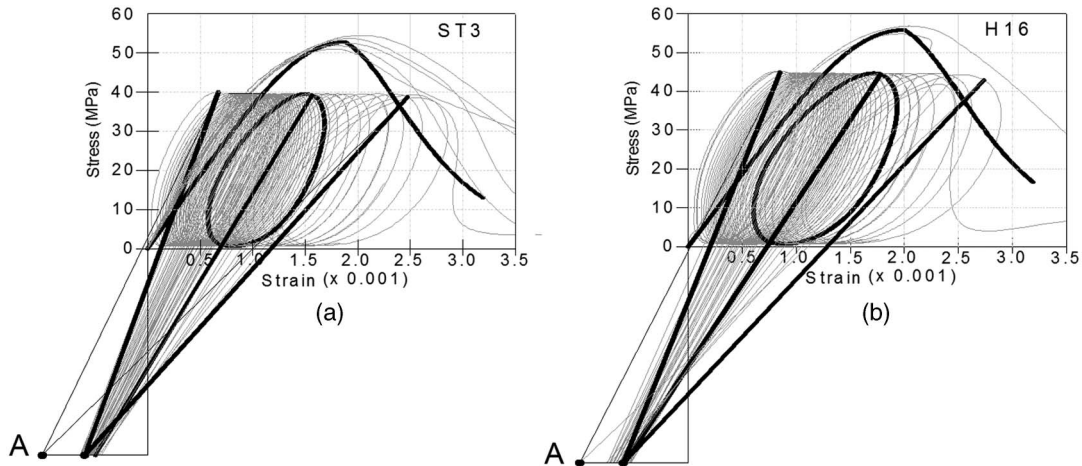
Fig. 3. Specimens in damaged states

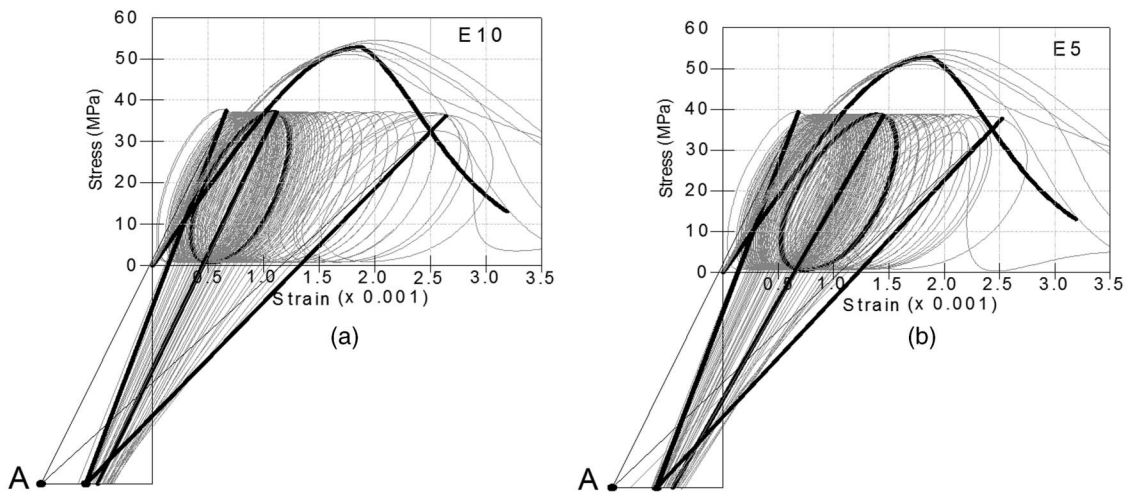**Fig. 4.** Fatigue degradation for ST3 ($f'_c = 52.8$ MPa) and H16 ($f'_c = 55.8$ MPa)

Fig. 5. Fatigue degradation for E5 ($f'_c = 52.8$ MPa) and E10 ($f'_c = 52.8$ MPa)

the stress–strain envelopes required to verify the intersection of the peak stresses for the statically loaded fatigue-damaged specimens. However, the stress–strain curves obtained from the experiments were also included in the plots.

Failure Modes

Fig. 3 shows specimens in various damaged states. In all, hairline cracks parallel to the applied loading direction were initially observed. Thereafter, the cracks widened and finally failed in the form of faults.

Experimental Results and Verification

Fatigue Degradation

The fatigue stress–strain hysteresis loops for the concrete cylinders tested are shown in Figs. 4–7 for some tested specimens. The
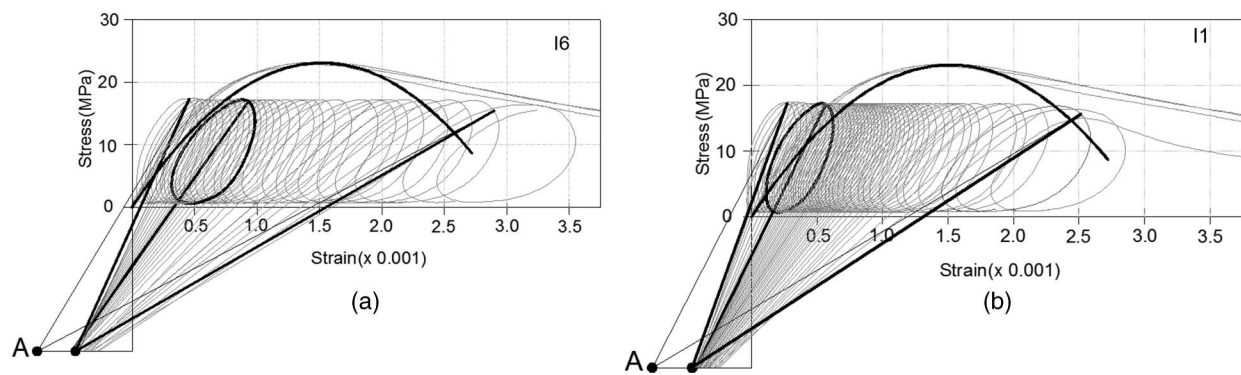
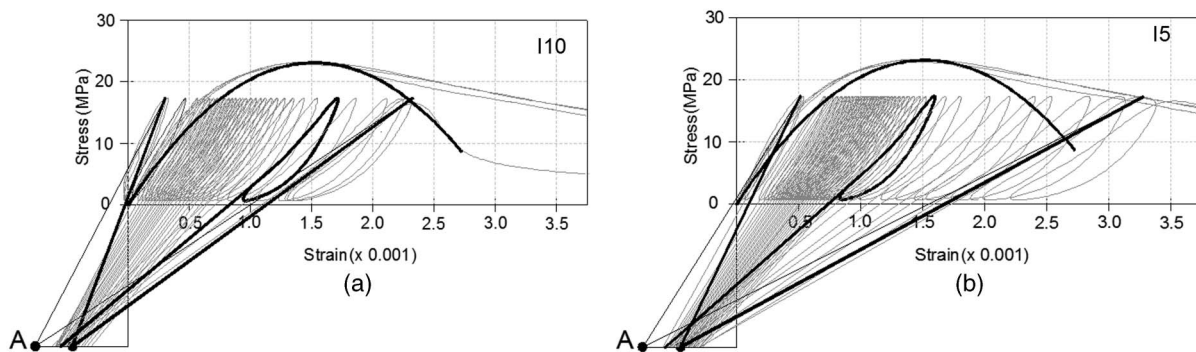**Fig. 6.** Fatigue degradation for I1 and I6 ($f'_c = 23.1$ MPa) at 5 Hz

Fig. 7. Fatigue degradation for I6 and I5 ($f'_c = 23.1$ MPa) at 1 Hz

monotonic stress–strain curves obtained from the experiments conducted and from Popovics' equation for high-strength concrete ($\geq$40 MPa) were plotted as envelopes for the hysteresis loops. In the case of normal-strength concrete (<40 MPa), stress–strain curves generated from Hognestad's constitutive equation were used.

The fatigue hysteresis loops for each tested specimen were plotted using stress–strain values at intervals of cycles. As the specimen degradation became substantial, the intervals were reduced.

From the experiment plots, the shapes of the hysteresis loops at a loading frequency of 5 Hz were observed to be fully developed ellipses (Figs. 4–7). The sizes increased progressively with a corresponding increase in loading cycles. However, towards failure, the elliptical shapes were distorted. The centerline for each hysteresis loop was further extended along the approximate major axes (Figs. 4–6). On the other hand, the shapes of the hysteresis loops obtained from tests conducted at a frequency of 1 Hz were initially elliptical with smaller minor axes. As the number of cycles increased, the reloading paths of the curves were approximately linear and subsequently became concave with further increase in the number of cycles (Fig. 7). This observation reveals the influence of the loading frequency on the shapes of the fatigue hysteresis loops for plain concrete in compression.
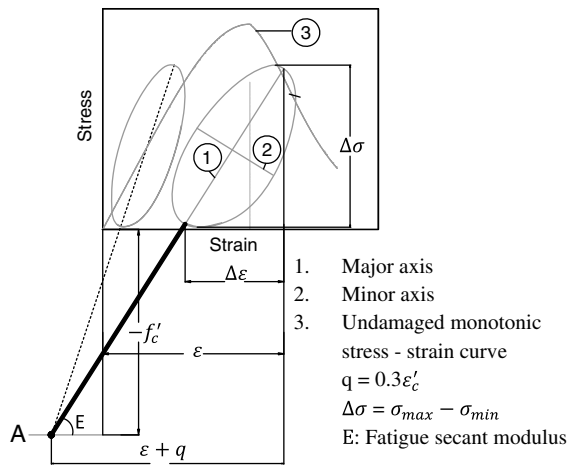
From Figs. 4–7, the last hysteresis loop at failure approached or intersected the softening portion of the stress–strain envelope. Generally, each last loop evolved between the softening portion of the experimental stress–strain curve and the stress–strain models used (Popovics' and Hognestad's). Hence, the assumption of the intersection of the last loop with the softening portion of the stress–strain envelope can be considered realistic.

In order to verify the assumption proposed by Park (1990), the centerline of each hysteresis loop plotted was extended to cross a horizontal line drawn at an ordinate of $-f'_c$ (where f'_c is the compressive strength value) as shown in Figs. 4–7. The required slopes (fatigue secant moduli) for the hysteresis loops with concave reloading paths were obtained by extending centerlines drawn between ordinate points ($0.25f'_c$) and tangents at lower points on the hysteresis loops.
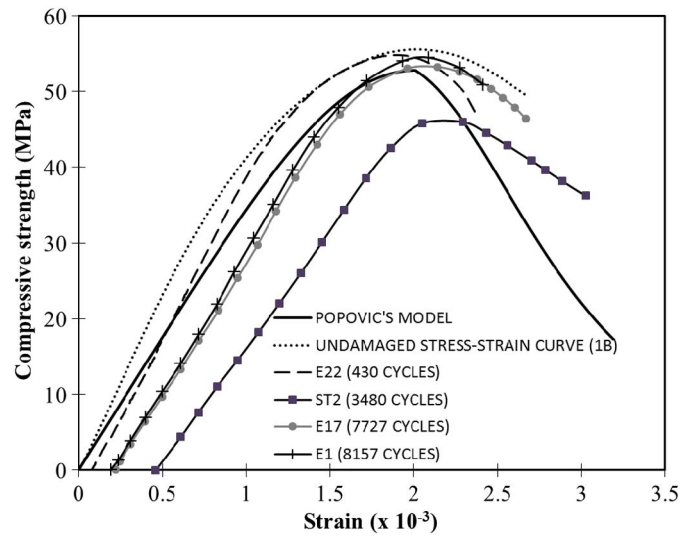
Point A indicated in the figures, with a coordinate of ($-0.5\varepsilon'_c$, $-f'_c$) (where ε'_c is the strain corresponding to the peak stress), corresponds to the convergence point proposed by Park (1990). As observed, Park's convergence point underestimates the fatigue modulus of degraded concrete. This is due to the assumption that the initial concrete fatigue secant modulus is equal to the static secant modulus. Based on the observed results, the fatigue secant modulus of concrete is generally higher than the static secant modulus. From the observed hysteresis loops (Figs. 4–7), the initial centerline meets a coordinate point approximately ($-0.3\varepsilon'_c$, $-f'_c$). Subsequent centerlines deviate from the point as irreversible strain accumulates. As the damage becomes substantial (more inclined loops), the centerlines tend towards the initial convergence point. Hence, from the geometry of the stress–strain plots (Figs. 8 and 9), an assumed convergence point of ($-0.3\varepsilon'_c$, $-f'_c$) is proposed.
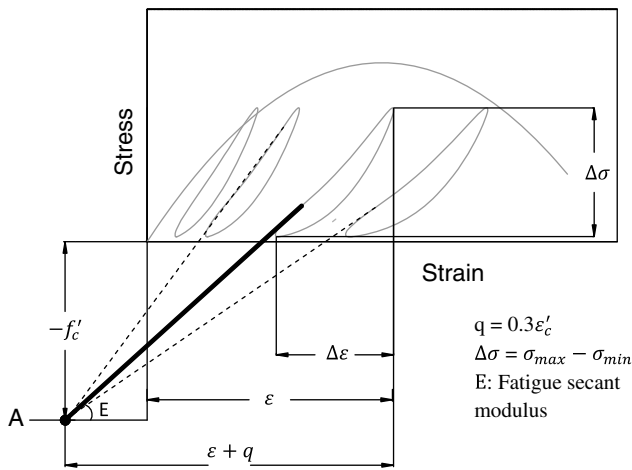
Irreversible Strain under Fatigue Loading

The irreversible strain at a given cycle is equal to the strain corresponding to the minimum stress level at that cycle. Initially, the centerlines intersected the hysteresis loops at points corresponding to the minimum stress point on each hysteresis loop (Figs. 8 and 9).

© ASCE

04017028-5

J. Mater. Civ. Eng.

Fig. 8. Fatigue degradation (high frequency)

1. Major axis
2. Minor axis
3. Undamaged monotonic stress - strain curve

$q = 0.3\varepsilon_c'$

$\Delta\sigma = \sigma_{max} - \sigma_{min}$

E: Fatigue secant modulus

$q = 0.3\varepsilon_c'$

$\Delta\sigma = \sigma_{max} - \sigma_{min}$

E: Fatigue secant modulus

Fig. 9. Fatigue degradation (low frequency)

As the cycles increased, the distance between each centerline and the point corresponding to the minimum stress level on the fatigue hysteresis loops increased progressively. This is attributed to the subsequent inclination of the loops and a strain evolution due to the minimum applied stress under static condition.
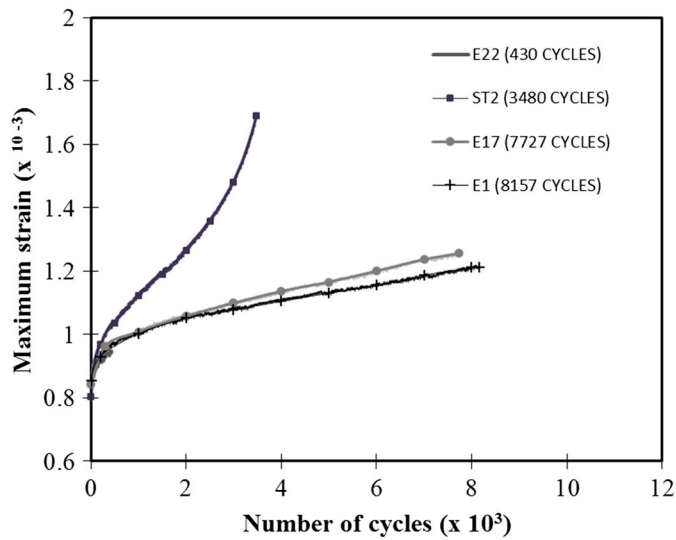
The strain due to the minimum stress level under static conditions (lower turning point of fatigue loading) is a function of the static secant modulus evolution. However, at zero minimum stress level, the value is null. Based on the proposed assumption and from the geometries in Fig. 8 or 9, a model was proposed for the irreversible fatigue strain (ε_d) as follows.

For $0.3N_f \leq N \leq N_f$ (where N_f = number of cycles to failure and N = number of fatigue loading cycles)
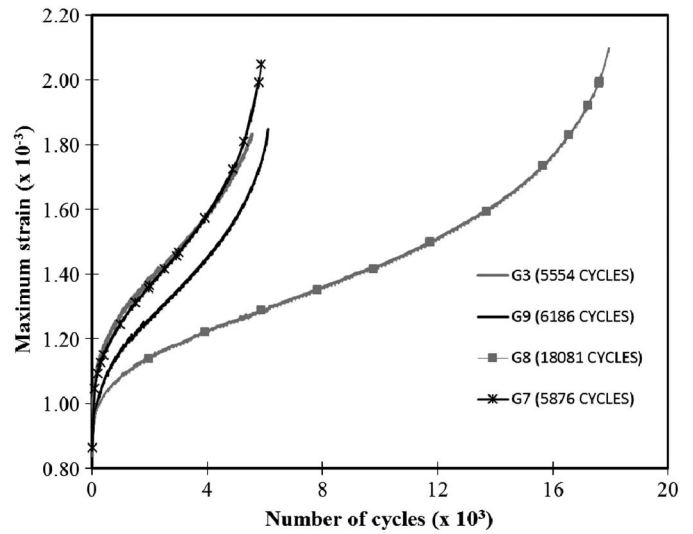
$$\varepsilon_d = \varepsilon - \Delta\varepsilon \qquad (1)$$

where $\varepsilon_d = \varepsilon_{d0} + \varepsilon_{d1} + \varepsilon_{d2}$; $\Delta\varepsilon$ = fatigue strain range; ε_{do} = strain due to loops centerlines convergence; ε_{d1} = strain due to the hysteresis loop inclination; and ε_{d2} = strain due to the minimum stress at the turning point of fatigue loading
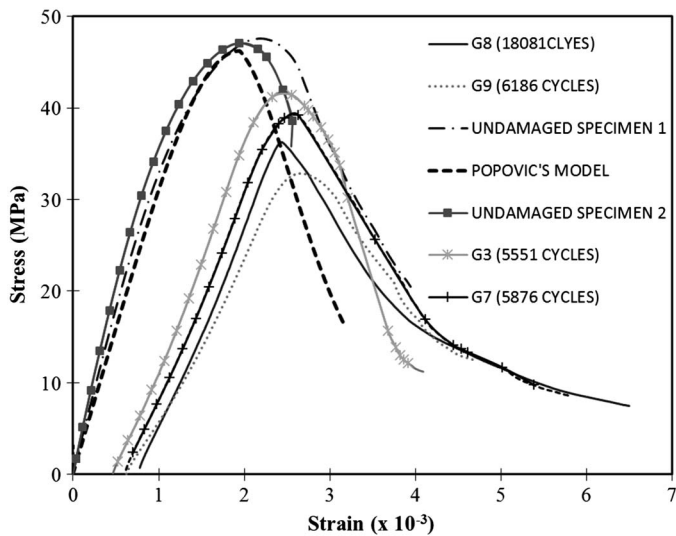
$$\varepsilon_{do} = -\left[\frac{f_c' + (\sigma_{max}R)}{E}\right] - 0.3\varepsilon_c' \qquad (2)$$

Fig. 10. Residual strength (Batch 1)

$$\varepsilon_{d1} = -k_2 q \left(\frac{D_{fc}}{\sqrt{D_{ce}}}\right) \qquad (3)$$

$$\varepsilon_{d2} = \frac{-(\sigma_{max}R)}{E_{sec}} \qquad (4)$$

where E = fatigue secant modulus; $k_2 = 1.0$ for high-strength concrete and 2.0 for normal-strength concrete; q in Figs. 8 and 9 = $0.3\varepsilon_c'$; R = stress ratio; σ_{max} = maximum stress level; and E_{sec} = degraded static secant modulus. The models for D_{fc} (concrete strength damage) and D_{ce} (fatigue secant modulus damage) used were previously proposed by Isojeh (2016).

As reported in the literature, the first stage of deformation under fatigue loading is characterized by cyclic creep. As such, the irreversible strain for any number of cycles less than 30% of the cycles leading to failure (N_f) is estimated as a function of the irreversible strain at 0.3, where the irreversible strain at 0.3 is estimated using Eqs. (1)–(4). Hence, for $N < 0.3N_f$

$$\varepsilon_d = \varepsilon_{d3}\left(\frac{N}{0.3N_f}\right)^\delta \qquad (5)$$

where ε_{d3} = irreversible strain (ε_d) value at $0.3N_f$. The value of δ (fatigue creep constant) can be taken as 0.3. The implementation of the irreversible strain model into constitutive models for normal-strength and high-strength concrete will be discussed in a subsequent section.

Strength Degradation

The results of the 22 cylindrical specimens tested for strength degradation are presented in Table 3. Figs. 10–15 show the residual strengths and corresponding strain evolutions after loading each specimen to the number of cycles specified in Table 3. As observed from the stress–strain plots shown in Fig. 10 and the maximum strain evolution plots shown in Fig. 11, an obvious degradation of concrete strength began after a substantial number of cycles had been applied to a specimen, as in the case of Specimen ST2.

From Figs. 10 and 11, there was no obvious strength deterioration within the primary phase and within a large portion of the secondary phase of damage for the strain evolution. The obvious strength deterioration in Specimen ST2 corresponds to the tertiary
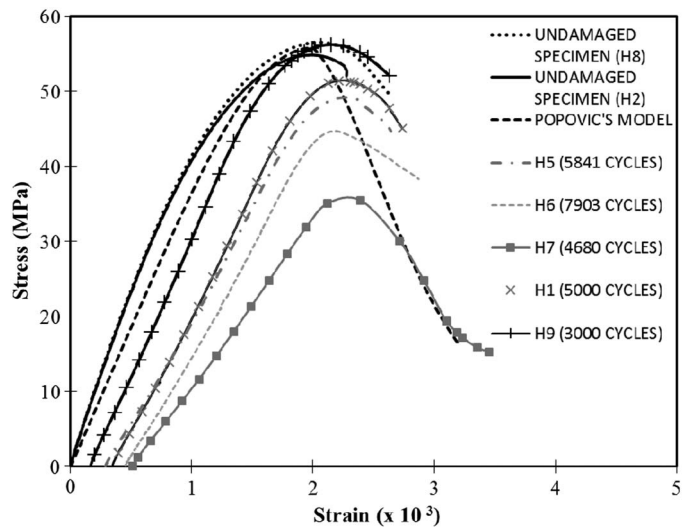
Fig. 11. Strain evolution corresponding to residual strength for Batch 1

Fig. 13. Strain evolution corresponding to residual strength for Batch 2

Fig. 12. Residual strength (Batch 2)

Fig. 14. Residual strength (Batch 3)

stage of damage. From Figs. 10, 12, and 14, the assumption that the peak stress of the degraded stress–strain curve after fatigue loading intersects the stress–strain curve envelop at a point on the softening portion is considered reasonable.
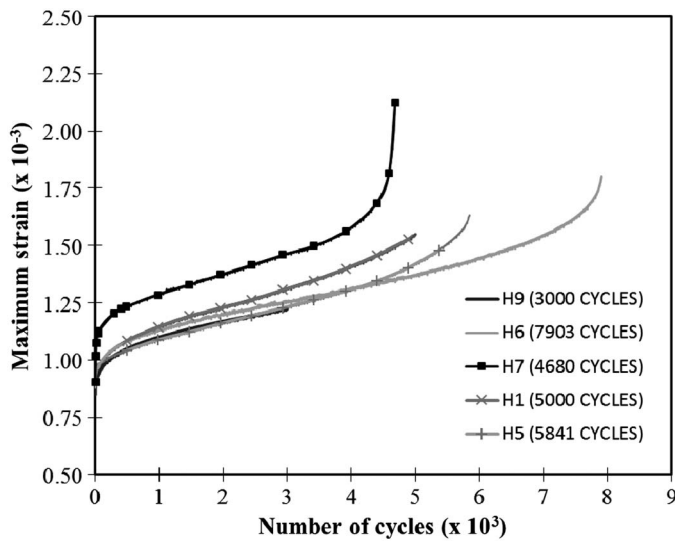
Ratio of the Fatigue Secant Modulus to Static Secant Modulus

In Eqs. (2)–(4), the static (E_{sec}) and fatigue (E) secant moduli are required in estimating the irreversible strain. Although it can be assumed that the damage evolutions for both parameters are the same, the relationship between these parameters were verified to augment the assumption. The ratio of the fatigue secant modulus to the static secant modulus for each of the 22 specimens tested were further estimated and plotted against the corresponding normalized fatigue cycles given in Table 3. Fig. 16 and Eqs. (6) and (7) describe the procedure for estimating the static and fatigue secant moduli of concrete, E and E_{sec}, respectively, for each of the 22
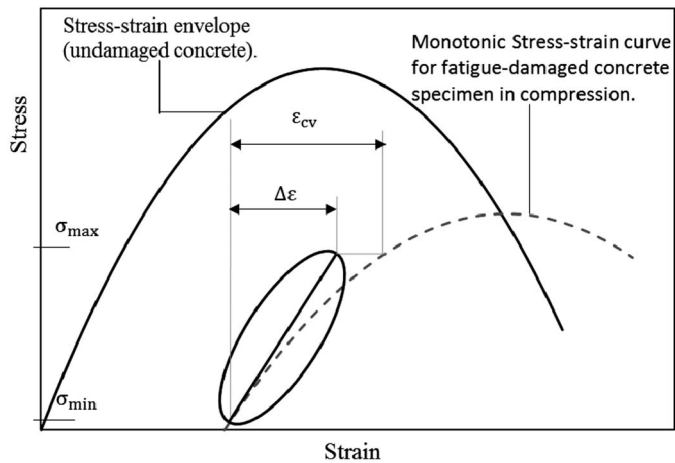
specimens tested. The results are shown in Fig. 17. From Fig. 17, it can be observed that the ratios are fairly constant throughout the evolution and the damage evolution for both are similar. Hence, the value of the ratio of the fatigue secant modulus to the static secant modulus can be assumed between 1.3 and 1.6. Based on this observation, and provided that the initial static secant modulus for concrete is known, the value of the fatigue secant modulus can be taken as 1.5 and 1.45 times the static secant modulus for high-strength and normal-strength concrete, respectively. In Eqs. (6) and (7), σ_{min} = minimum stress level; $\Delta\varepsilon$ = fatigue strain range; and ε_{cv} = strain corresponding to the stress range ($\sigma_{max} - \sigma_{min}$) on the monotonic stress–strain curve

$$E = \frac{\sigma_{max} - \sigma_{min}}{\Delta\varepsilon} \tag{6}$$

$$E_{sec} = \frac{\sigma_{max} - \sigma_{min}}{\varepsilon_{cv}} \tag{7}$$

Fig. 15. Strain evolution corresponding to residual strength for Batch 3

Fig. 17. Plot of the ratio of the fatigue secant modulus (E) to the static secant modulus against a normalized number of cycles

Fig. 16. Static and fatigue secant moduli

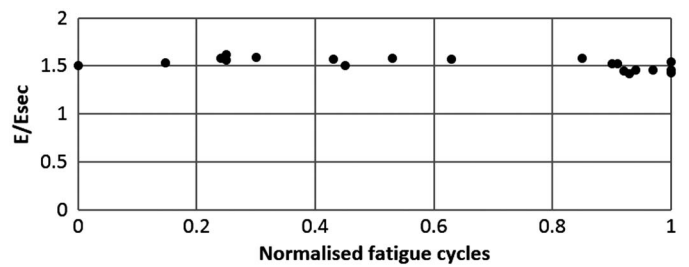**Fig. 18.** Modified Hognestad's stress–strain curve for damaged concrete

Damaged Constitutive Models for Residual Strength of Concrete
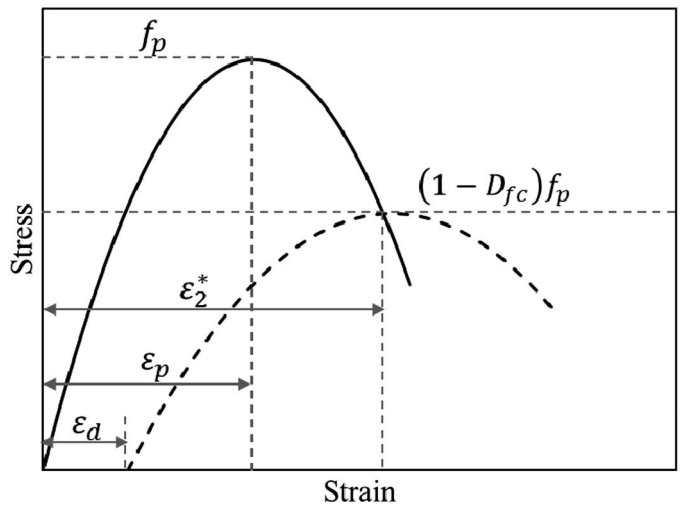
Normal-Strength Concrete

The Hognestad stress–strain curve for normal strength is used for estimating the effective stress of a concrete element under a monotonic loading, provided the concrete peak stress (or compressive strength), induced effective strain, and the strain corresponding to the peak stress are known. Based on the assumption of the intersection of the peak stress of a damaged concrete specimen with the softening portion of the stress–strain envelope, the Hognestad parabolic equation can be used to obtain the strain corresponding to the degraded strength and, as such, a damage constitutive model can be developed for concrete under fatigue loading by modifying the peak strength and the strain corresponding to the peak stress (Fig. 18). The Hognestad's equation is modified thus

$$\left(\frac{\varepsilon_{c2}}{\varepsilon_p}\right)^2 - \frac{2\varepsilon_{c2}}{\varepsilon_p} + \frac{f_{c2}}{f_p} = 0 \tag{8}$$

where f_{c2} = principal compressive stress; f_p = peak concrete compressive stress (equal to f'_c); ε_p (equal to ε'_c) = compressive strain

corresponding to f_p; and ε_{c2} = average net strain in the principal compressive direction.

Based on the assumption $(1 - D_{fc})f_p = f^*_c$, and $f_{c2} = f^*_c$

$$\left(\frac{\varepsilon^*_2}{\varepsilon_p}\right)^2 - \frac{2\varepsilon^*_2}{\varepsilon_p} + \frac{(1 - D_{fc})f_p}{f_p} = 0 \tag{9}$$

$$\left(\frac{\varepsilon^*_2}{\varepsilon_p}\right)^2 - \frac{2\varepsilon^*_2}{\varepsilon_p} + (1 - D_{fc}) = 0 \tag{10}$$

where ε^*_2 = total strain at peak stress intersection point with the stress–strain envelope; and f^*_c = degraded concrete strength.

Solving the equation for the total strain corresponding to the new degraded strength gives

$$\varepsilon^*_2 = \varepsilon_p(1 + \sqrt{D_{fc}}) \tag{11}$$

From Fig. 18, it can be observed that the value of ε^*_2 also includes the strain offset (ε_d), hence the strain corresponding to the peak stress of the degraded concrete strength ε^*_c is given as

$$\varepsilon^*_c = \varepsilon^*_2 - \varepsilon_d \tag{12}$$

$$\varepsilon^*_c = \varepsilon_p(1 + \sqrt{D_{fc}}) - \varepsilon_d \tag{13}$$

where ε_d can be obtained from Eqs. (2)–(4); ε_p = concrete compressive strain corresponding to the peak stress of undamaged
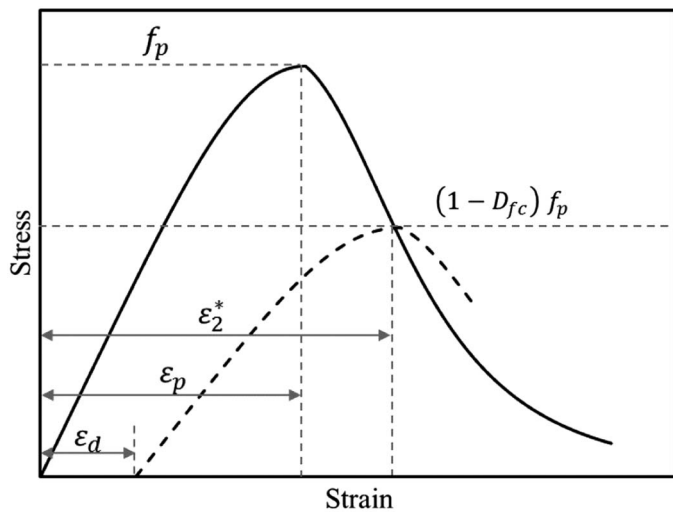
Fig. 19. Modified Popovic's stress–strain curve for damaged concrete

Fig. 21. Irreversible fatigue strain for normal-strength concrete

Fig. 20. Irreversible fatigue strain for high-strength concrete (stress level: 0.74)

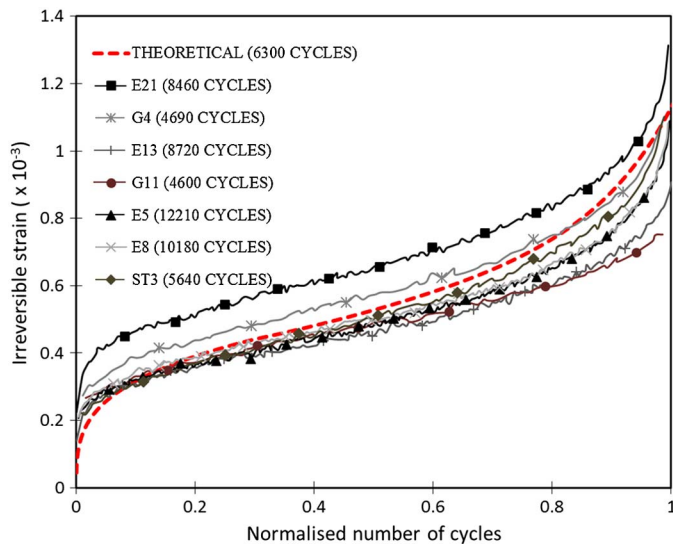concrete; and D_{fc} (concrete strength damage) can be estimated as described by Isojeh (2016).
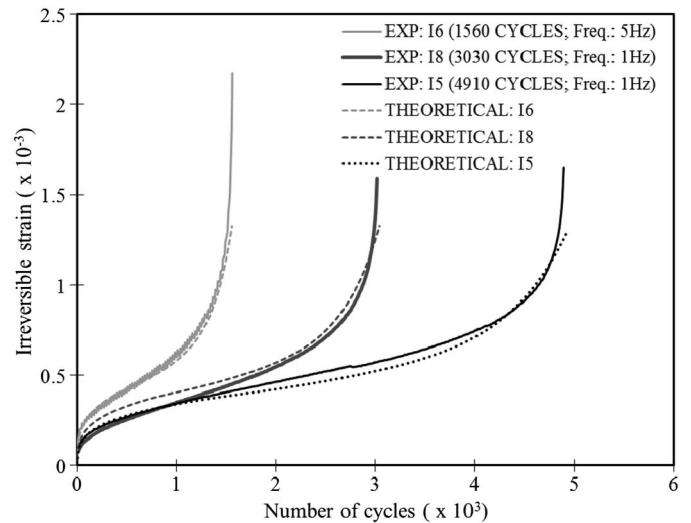
High-Strength Concrete

Popovics' stress–strain model was modified for fatigue-damaged concrete for high-strength concrete. The approach is similar to that for normal-strength concrete (Fig. 19). However, to obtain the strain corresponding to the degraded strength, an iterative method is required such as the Newton-Raphson method; thus

$$f_{c2} = f_p \frac{n(\varepsilon_{c2}/\varepsilon_p)}{(n-1) + (\varepsilon_{c2}/\varepsilon_p)^{nk}} \quad (14)$$

where, according to Collins et al. (1997)

$$n = 0.80 - f_p/17 (\text{in MPa}) \quad (15)$$

$$k = 0.6 - \frac{f_p}{62} \quad \text{for } \varepsilon_{c2} < \varepsilon_p < 0 \quad (16)$$

where n = curve-fitting parameter for stress–strain response of concrete in compression; and k = postdecay parameter for stress–strain response of concrete in compression.

From Eq. (14), $\varepsilon_{c2}/\varepsilon_p$ can be assumed to be t and $f_{c2} = (1 - D_{fc})f_p$; hence

$$(1 - D_{fc}) = \frac{nt}{(n-1) + t^{nk}} \quad (17)$$

$$f(t_i) = \text{Rearranging, } n - 1 + t^{nk} - \frac{nt}{(1 - D_{fc})} \quad (18)$$

Using Newton-Raphson's method and differentiating Eq. (18) with respect to t yields

$$m' = nkt^{nk-1} - \frac{n}{(1 - D_{fc})} \quad (19)$$

where m' = differentiation of Eq. (18)

$$t_{i+1} = t_i - \frac{f(t_i)}{m'} \quad (20)$$

where t_i = initial value of t assumed; and t_{i+1} = value of the next step computed using Eq. (20). Provided $|(t_{i+1} - t_i)/t_i|$ is small enough, then the value of $t = t_{i+1}$. Hence, ε_2^* and ε_c^* can be obtained as described for normal concrete and in Fig. 19.

Verification of Proposed Model for Irreversible Strain

The model developed for fatigue irreversible strain was corroborated using experimental results from Batches 1 and 4 for high-strength and normal-strength concrete, respectively. The irreversible strain evolution for seven high-strength concrete specimens, tested under fatigue loading at a maximum stress level and minimum force of 0.74 and 5 kN, respectively, were plotted as shown in Fig. 20. The specimens were all tested at a frequency of 5 Hz.

STEP 1

From static analysis, estimate the initial stress (f_{c2max}) and (f_{c2min}) (maximum and minimum stress levels), and the initial static secant modulus; modify the value for the initial fatigue secant modulus using appropriate factors.

STEP 2

Estimate the number of cycles to failure due to the applied stresses and the loading conditions (frequency, waveform), using the modified model by Zhang et al. (1998).

STEP 3

Estimate the strength and secant modulus damage at $0.3N_f$ and for the required cycle (s) as illustrated in Isojeh et al. "[Concrete damage under fatigue loading in uniaxial compression]"

STEP 4

Estimate the irreversible strain using Equations 2 to 5 for the first cycle. For subsequent cycles under constant fatigue loading, go to

For variable fatigue loading, go to

For both cases of loading, the previous damage before the next cycle should be converted to an equivalent cycle, as illustrated in Isojeh et al. "[Concrete damage under uniaxial compression],"

Fig. 22. Steps for estimating the irreversible strain of concrete under fatigue loading in compression

Fig. 21 shows the irreversible strain plot for normal-strength concrete specimens. As previously indicated, the irreversible strain model incorporates a residual strength and secant modulus damage models, which, in turn are functions of loading parameters such as frequency. Specimens I5 and I8 were tested at a frequency of 1 Hz, while Specimen I6 was tested at 5 Hz. Due to the stochastic nature of concrete observed in the number of cycles to failure at a stress level of 0.75, the maximum stress level corresponding to the number of cycles at failure was estimated for each specimen using a backward approach from Zhang et al.'s (1998) S-N model. The stress levels for Specimens I5, I8, and I6 were observed to be 0.73, 0.75, and 0.8, respectively. Each stress level was further used to estimate the progressive damage for residual strength and secant modulus per cycle and implemented into Eqs. (2)–(5) for each cycle. The procedure for estimating the irreversible strain is described subsequently in Fig. 22. A program was written to generate the irreversible strain per loading cycle.

Summary

From the investigations conducted, the following can be deduced:
- The intersections of the fatigue hysteresis at failure and the stress–strain curve of a fatigue-damaged concrete with the stress–strain envelope were found to be realistic, taking into account the well-known stochastic behavior of concrete. However, the common point at which the centerlines of fatigue hysteresis loops converge required modification in order to enhance the simplified constitutive model;
- Having observed the fact that the fatigue secant modulus is generally higher than the corresponding static secant modulus, a more-appropriate fatigue-deformation prediction can be obtained using the modified convergence coordinate proposed;
- The conducted investigation shows the influence of the loading frequency on the shape of the fatigue hysteresis loops. This should be accounted for in any hysteresis loop model. However, since high-cycle fatigue loading involves many hysteresis loops, expressing the fatigue behavior of concrete using maximum deformation evolutions saves computation time;
- Using the proposed constitutive models for concrete under fatigue loading, the deformation evolution of a concrete element can be estimated per cycle since the progressive damage of concrete strength and stiffness, and the irreversible strain accumulation are accounted for;
- There is a reasonable correlation between the theoretical and the experimental plots for the irreversible strains. As such, the proposed irreversible-strain models can be used for estimating the

required fatigue prestrain, provided the progressive variation in loading is taken into account; and

- More investigation on the implementation of the proposed models into the fatigue analysis of reinforced concrete structures is required in order to study the interaction between fatigue-damaged concrete and other constituent materials.

Acknowledgments

Notation

The following symbols are used in this paper:

D_{ce} = damage value for fatigue secant modulus;
D_{fc} = damage value for concrete strength;
E = fatigue secant modulus;
E_{Sec} = static secant modulus;
F = frequency
f_{c2} = principal compressive stress;
f_p = peak concrete compressive stress;
f_c' = compressive strength;
f_c^* = degraded compressive strength;
K = postpeak decay parameter for stress–strain response of concrete in compression;
k_2 = strain factor (1.5 for high-strength concrete and 1.45 for normal-strength concrete);
N = number of cycles;
N_{eqv} = equivalent cycles;
N_f = numbers of cycles at failure;
n = curve-fitting parameter for stress–strain response of concrete in compression;
Q = abscissa of proposed convergence point;
R = stress ratio;
S_{max} = maximum stress level;
$\Delta\varepsilon$ = fatigue strain range;
Δf = maximum stress level;
δ = fatigue creep constant;
ε = total fatigue strain;
ε_{c2} = average net concrete axial strain, in the principal compressive direction;
ε_{cv} = strain corresponding to the stress range $(\sigma_{max} - \sigma_{min})$ using the monotonic stress–strain curve;
ε_c' = strain corresponding to peak stress;
ε_d = irreversible fatigue strain;
ε_{do} = irreversible strain due to loops centerlines convergence;
ε_{d1} = irreversible strain due to the hysteresis loop inclination;
ε_{d2} = irreversible strain due to the minimum stress level under static condition;
ε_{d3} = irreversible strain at $0.3N_f$;
ε_2^* = total strain at peak stress intersection point with stress–strain envelope;
ε_p = concrete compressive strain corresponding to f_p;
σ_{max} = maximum stress level; and
σ_{min} = minimum stress level.

References

Al-Gadhib, A. H., Baluch, M. H., Shaalan, A., and Khan, A. R. (2000). "Damage model for monotonic and fatigue response of high strength concrete." *Int. J. Damage Mech.*, 9(1), 57–78.

Cachim, P. B., Figueiras, J. A., and Pereira, P. A. A. (2002). "Fatigue behaviour of fibre-reinforced concrete in compression." *Cem. Concr. Compos.*, 24(2), 211–217.

Chaboche, J. (1981). "Continuum damage mechanics: A tool to describe the phenomena before crack initiation." *Nucl. Eng. Des.*, 64(2), 233–247.

Chaboche, J. (1988a). "Continuum damage mechanics. Part I: General concepts." *J. Appl. Mech.*, 55(1), 59–72.

Chaboche, J. (1988b). "Continuum damage mechanics. Part II: Damage growth, crack initiation, and crack growth." *J. Appl. Mech.*, 55(1), 59–72.

Collins, M. P., and Mitchell, D. (1997). *Prestressed concrete structures*, Response Publications, Toronto and Montreal.

Dafalias, Y. F., and Popov, E. P. (1977). "Cyclic loading for materials with a vanishing elastic region." *Nucl. Eng. Des.*, 41(2), 293–302.

Eligehausen, R., Kazic, M., and Sippel, T. M. (1992). "Creep and fatigue analysis of reinforced concrete structures." *Proc., Riga, Latvia, Int. Conf. Bond in Concrete from Research to Practice*, Riga Technical Univ., Riga, Latvia.

Hognestad, E. (1951). "A study on combined bending and axial load in reinforced concrete members." *University of Illinois Engineering Experiment Station*, Univ. of Illinois, Urbana-Champaign, IL, 43–46.

Holmen, J. O. (1982). "Fatigue of concrete by constant and variable amplitude loading." *ACI SP* 75(4), 71–110.

Isojeh, B. (2016). "Fatigue behaviour of steel fibre concrete in direct tension." *ACI Mater. J.*, in press.

Isojeh, B., El-Zeghayar, M., and Vecchio, F. J. (2016). "Concrete damage under fatigue loading in uniaxial compression." *ACI Mater. J.*, in press.

Karsan, I. D., and Jirsa, J. O. (1969). "Behaviour of concrete under compressive loadings." *J. Struct. Div.*, 95(12), 2543–2563.

Lemaitre, J. (1986). "Local approach of fracture." *J. Eng. Fract. Mech.*, 25(5–6), 523–537.

Lemaitre, J., and Chaboche, J. L. (1990). *Mechanics of solid materials*. Cambridge University Press, Cambridge, U.K.

Medeiros, A., et al. (2015). "Effect of the loading frequency on the compressive fatigue behavior of plain and fiber reinforced concrete." *Int. J. Fatigue*, 70, 342–350.

Otter, D. E., and Naaman, A. E. (1989). "Model for response of concrete to random compressive loads." *J. Struct. Eng.*, 10.1061/(ASCE)0733 -9445(1989)115:11(2794), 2794–2809.

Park, Y. J. (1990). "Fatigue of concrete under random loadings." *J. Struct. Eng.*, 10.1061/(ASCE)0733-9445(1990)116:11(3228), 3228–3235.

Petryna, Y. S., Pfanner, D., Stangenberg, F., and Kratzig, W. B. (2002). "Reliability of reinforced concrete structures under fatigue." *Reliab. Eng. Syst. Saf.*, 77(3), 253–261.

Popovics, S. (1970). "A review of stress–strain relationships for concrete." *ACI J.*, 67(3), 243–248.

Raithby, K. D., and Galloway, J. W. (1974). "Effects of moisture condition, age and rate of loading on fatigue of plain concrete." *ABELES Symp.*, American Concrete Institute, Detroit, 15–34.

Sparks, P. R., and Menzies, J. B. (1973). "The effect of rate of loading upon the static and fatigue strength of plain concrete in compression." *Mag. Concr. Res.*, 25(83), 73–80.

Su, E. C. M., and Hsu, T. T. C. (1988). "Biaxial compression fatigue and discontinuity of concrete." *ACI Mater. J.*, 85(3), 178–188.

Suaris, W., Ouyang, C., and Fernando, V. M. (1990). "Damage model for cyclic loading of concrete." *J. Eng. Mech.*, 10.1061/(ASCE)0733-9399 (1990)116:5(1020), 1020–1035.

Tamulenas, V., Gelazius, V., and Ramanauskas, R. (2014). "Calculation technique for stress–strain analysis of RC elements subjected to high-cycle compression." *Mokslas: Lietuvos Ateitis*, 6(5), 468–473.

Torrenti, J. M., Pijaudier-Cabot, G., and Reynouard, J. (2010). *Mechanical behaviour of concrete: Cyclic and dynamic loading, fatigue of structural concrete*, ISTE and Wiley, Hoboken, NJ, 185–223.

Vega, I. M., Bhatti, M. A., and Nixon, W. A. (1995). "A nonlinear fatigue damage model for concrete in tension." *Int. J. Damage Mech.*, 4(4), 362–379.

Xiang, T., and Zhao, R. (2007). "Reliability evaluation of chloride diffusion in fatigue damaged concrete." *Eng. Struct.*, 29(7), 1539–1547.

Zanuy, C., Fuente, P., and Albajar, L. (2007). "Effect of fatigue degradation of the compression zone of concrete in reinforced concrete sections." *Eng. Struct.*, 29(11), 2908–2920.

Zhang, B., et al. (1996). "Effects of loading frequency and stress reversal on fatigue life of plain concrete." *Mag. Concr. Res.*, 48(177), 361–375.

Zhang, B., Phillips, D. V., and Green, D. R. (1998). "Sustained loading effect on the fatigue life of plain concrete." *Mag. Concr. Res.*, 50(3), 263–276.

Zhang, W., and Cai, Y. (2010). "Continuum damage mechanics and numerical applications." Springer, Heidelberg, Germany.

Zuradzka, S. S. (2008). *Fatigue strength of concrete under sulphate attack*, Cracow Univ. of Technology, Cracow, Poland, 31–155.